FRACTURE AND DISPERSION OF SELECTED CERAMICS UNDER EXPLOSIVE LOADS

Q. Wu[1], K.M. Jaansalu[2], W.S. Andrews[1], L.S. Erhardt[3], G. Roy[4] and P. Brousseau[4]

[1]*Department of Chemistry and Chemical Engineering, Royal Military College of Canada, Kingston ON CANADA*

[2]*Department of Metallurgical and Materials Engineering, Montana Tech of the University of Montana, Butte, Montana USA 59701-8997*

[3]*Radiological Analysis and Defence Group, Defence R&D Canada-Ottawa, 3701 Carling Avenue, Ottawa, ON, CANADA, K1A 0Z4*

[4]*Defence R & D Canada-Valcartier, 2459 Pie-XI Blvd North, Val-Bélair, QC, CANADA G3J 1X5*

A research program has been started as part of Canada's Chemical Biological Radiological and Nuclear Research and Technology Initiative to assess the potential effects of 'dirty bombs'. This study focuses on the fine ceramic fragments, 1 to 10 μm in diameter, generated by an explosion that can be transported some distance. The particle fragment distributions are fit to a fragment distribution model from the literature that accounts for the distribution of defects and crack branching in the fragmentation process. Two materials are used as surrogates: strontium titanate and cerium dioxide. The initial fragment size distributions are influenced by the grain size of the parent ceramic material. The fragments that remain airborne after detonation are generated by transgranular fracture arising from crack branching processes. A larger grain size results in a larger number of fragments in the range of interest.

1. INTRODUCTION

To better understand the threat posed by radiological dispersal devices, or "dirty bombs," a research program has been initiated as part of Canada's Chemical Biological Radiological and Nuclear Research and Technology Initiative. The specific aims of the research, germane to this paper, involve investigating the explosive dispersal of

radiological material surrogates. In this study, non-radioactive ceramic materials have been used in place of radioactive materials.

Fragmentation of ceramic materials has applications in ballistics and mining, but most attention is paid to the large, or primary, fragments. This study focuses on those fragments that form an aerosol cloud and can be transported some distance. The size range of interest is 1 to 10 μm. Experimental data is collected in an indoor arena. Small explosive charges are attached to ceramic samples and the resulting fragments are collected by cascade impactors. Analysis of these fragments is leading to correlations involving material properties, explosive charge mass, and particle size distributions. A second aspect of the research involves the conduct of outdoor dispersion trials involving larger explosive charges. The resulting aerosol puff or debris cloud is tracked using a scanning lidar device that permits a spatial and temporal mapping of its evolution. The overall aim is to form a model capable of predicting the dispersion of a given ceramic material as a function of atmospheric conditions and explosive charge mass. This paper will focus on the characterization of the fragments and initial size distribution analysis of the aerosols generated in indoor trials.

2. BACKGROUND

Ceramic materials will fracture into large fragments and small particles when subjected to explosive loading. There are generally two types of fractures: crystal cleavage (transgranular) and grain boundary failure (intergranular). Due to the complex loading and rapid crack propagation, there may be several mechanisms occurring, resulting in different types of fractures at different length scales. The result is a distribution of fragment sizes. Commonly, only a single distribution function has been used to characterize the fragment sizes resulting from a given process; for example, the Gaudin- Schuhmann distribution in mineral comminution processing [1], or a power law distribution in impact fragmentation [2]. Recent literature reports that the fragment size distribution from exploding shells is found to be bimodal [3, 4]. It should not be a surprise that the size distribution shows a bimodal or multimodal distribution if each distribution arises from different physical mechanisms.

There are quite a few factors influencing the size distribution of fragments. One evident factor is the amount of input energy [5]. The type of fracture also determines the fragment sizes and the type of fracture is influenced by the bulk properties and microstructural characteristics of the material [6]. Additionally, larger fragments may break into smaller particles on collision (secondary fragmentation), or subsequently, smaller particles may adhere to each other and become larger particles (agglomeration).

There are several distribution functions in the literature that have been used for fragmentation. Åström et al [7] have developed a distribution function based on

fragment formation by two processes: random nucleation of cracks and crack branching. Cracks are nucleated at defects distributed around the material and form particles with sizes related to the distance between defects. Smaller particles arise due to a crack branching mechanism: as a crack rapidly propagates through a material, it forms side branches. These branches meet other cracks to form particles. The cumulative fragment distribution is then the sum of two terms:

$$\frac{N(s)}{N_T} = (1-\beta)s^{-\alpha}\exp\left(-s\left(2/\lambda\right)^D\right) + \beta\exp\left(\frac{-\left(s^{1/D}+\lambda\right)^D}{s_0}\right) \tag{1}$$

where N(s) is the cumulative number of particles larger than s, β is a weighting factor, λ is the penetration depth of the branching crack, s_0 is a constant relating to fragment size, and D is the dimensionality of the process. The parameter α is related to D:

$$\alpha = 2 - \frac{1}{D} \tag{2}$$

In this work, D is set to 3, and the adjusted parameters are N_T, β, λ, and s_0. The first term accounts for the particles generated by the crack branching mechanism, the second accounts for the particles generated by the distribution of defects in the material.

3. EXPERIMENTAL AND DATA COLLECTION

The detonation takes place in an enclosed arena, 2 m high by 6 m in diameter, using detasheet as the explosive. The ceramic pellet, either strontium titanate or cerium dioxide, is attached to a small charge (around 24 g) and detonated 1 meter above the floor. Cascade impactors collect the small ceramic fragments in the debris cloud after detonation. The impactors contain eight stages, each with a successively smaller cut-point diameter. The small fragments are removed from the air and sized as air is drawn through the device. The sampling position and time of cascade impactors are presented at Table 1 and the cut-point diameters are presented at Table 2. In the analysis of the distributions for each ceramic material, the data from two detonations are weight averaged.

Table 1. Running position and time of cascade impactors

Cascade impactor #	Height, m	Running Period
1	1	15 to 20 minutes after detonation
2	5	0 to 5 minutes after detonation

Table 2. Cut-point diameter (D_{50}) of each stage for cascade impactor.

Stage No.	1	2	3	4	5	6	7	8
Cut-point diameter (μm)	>21.3	14.8	9.8	6.0	3.5	1.55	0.93	0.52

The two materials used are strontium titanate and cerium dioxide and their properties are presented at Table 3. The density for both materials is as produced, both are at 95% of theoretical density. The elastic properties, measured using a standard impulse vibration technique, are not significantly different. Also characterized are the grain sizes within the produced material. The grain size distribution for the strontium titanate is skewed to the lower end, much more so than that for cerium dioxide. The lowest grain diameter observed for cerium dioxide is larger than the largest cut-point of the cascade impactors.

Table 3. Material properties

Material	Density ($g\ cm^{-3}$)	Young's Modulus (GPa)	Poisson's Ratio	Grain Size(μm) High	Low	Average
Strontium Titanate	4.862	187	0.20	50	8.9	24
Cerium Dioxide	6.772	182	0.32	73	23	47

4. RESULTS AND DISCUSSION

4.1 Particle Description

Filter sections from the cascade impactors are placed in a scanning electron microscope for particle characterization. Typical particles are shown in Figure 1. These particles exhibit facets and planes typical of transgranular fracture which is consistent with their sizes being much smaller than most of the grains observed in the material. In the case of cerium dioxide, there are several fine particles adhering to larger particles. This attachment of fine particles on the fragment surface may be due to opposite static charge. These charges may arise during the explosion from rapid fragmentation, collision, or dissociation of ions in the gas produced by the explosive. This agglomeration will then affect the size distribution within the debris cloud.

4.2 Particle size distributions

The particle size distributions are plotted at Figure 2 below. The mass fraction on each stage is plotted at the cut point diameter for that stage. For the strontium titanate, the distribution of fragments collected immediately after detonation (Impactor C2) follows a unimodal distribution. The fragments larger than 14.8 μm settle out of the debris cloud relatively quickly. The distribution sampled after fifteen minutes also

follows a unimodal distribution where a major fraction of these particles are smaller than smallest grain size observed in the material. The relatively high mass in the 9.8 μm interval may be due to the detonation completely liberating the smaller grains (≥ 8 μm) from the parent material. Alternatively, smaller fragments may be colliding and adhering to each other, or this is an artefact of the stage width of the impactor.

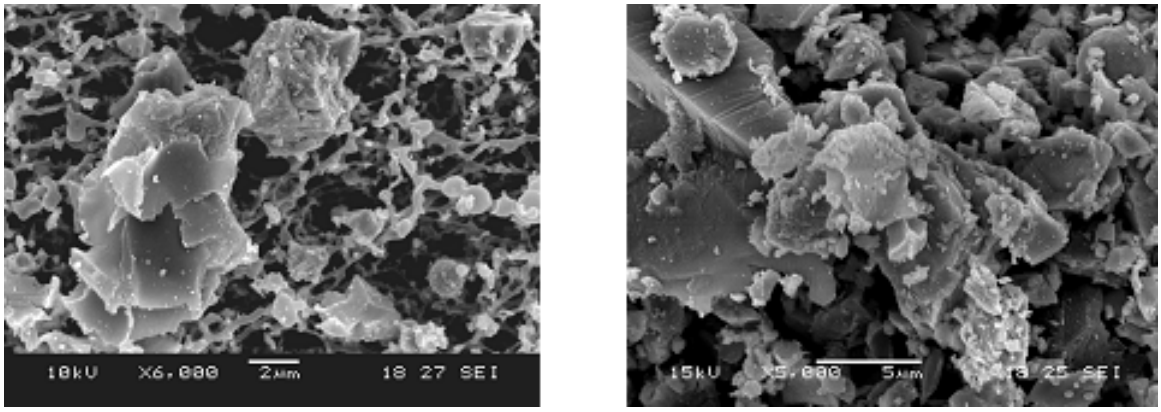

Figure 1: Typical particles from cascade impactors, left, strontium titanate, right, cerium dioxide.

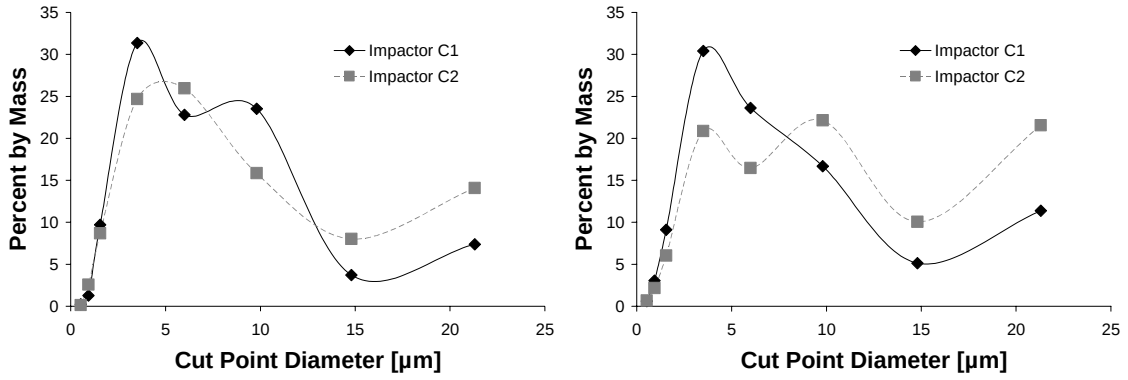

(a) (b)

Figure 2. Mass fraction vs size range: (a) strontium titanate and (b) cerium dioxide. Impactor 1 collects fragments for five minutes starting fifteen minutes after detonation. Impactor 2 collects fragments during a five minute period immediately after detonation.

Similar behaviour is seen with distributions within the debris cloud from the cerium dioxide. The distribution on detonation appears bimodal, and after the large particles have settled, the smaller fragments follow an exponential distribution. Here, a major fraction of the particles are much smaller than the smallest grain size (23 μm) of the parent material.

To determine a cumulative particle distribution, the number of particles on each stage is estimated from:

$$N(m_i) = \frac{m_i}{\rho V_i} \tag{3}$$

where m_i is the mass on i^{th} stage, ρ is the density of the material, and V_i is the volume of the average particle, calculated using the mid-point size of the collection range for that stage.

The cumulative distributions for strontium titanate are fit to equation (1) and the results and parameter values are presented in Figure 3. (In literature where equation 1 has been used to describe distributions of fractured rock, a small particle cut-off was applied to limit the size to the grain size of the material [8]. In this work, where the grains themselves have fractured, a small particle cut-off is not used.) On detonation, the value for s_0, 5.55 μm, is slightly smaller than the lower grain size observed of 8 μm. Intergranular fracture likely plays a role in the generation of these fragments. After fifteen minutes, the total number of particles has decreased and the distribution shifts to a smaller particle size as characterized by the value of s_0. In both cases, the value of β is unity. The penetration distance, λ, becomes smaller. The physical interpretation of λ is clear on detonation. For the second distribution, λ becomes a parameter that characterizes the finer fragments. This may be related to physical processes similar to a crack branching mechanism (eg microcracking) or to secondary fragmentation.

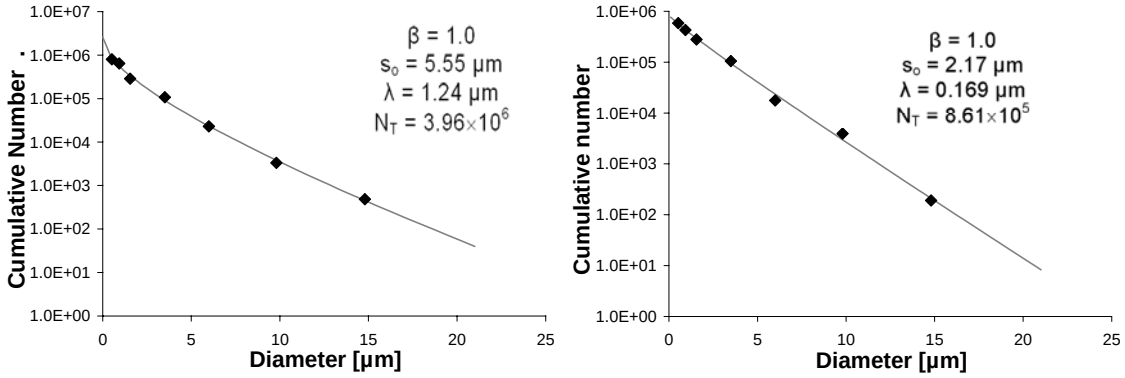

(a) (b)

Figure 3. The cumulative number aerosol distributions as a function of particle size for the strontium titanate for the five minute period (a) immediately after detonation (impactor C2) and (b) starting fifteen minutes after detonation (impactor C1).

The cumulative distributions and parameters for cerium dioxide are presented at Figure 4. The total number of fragments generated is larger: the mass of fragments collected by the impactors is roughly double the mass collected for strontium titanate

for a given explosive charge. On detonation, the fragment distribution is bimodal as β is 0.94. The value of s_0 is 20.74 μm, slightly smaller than the lower grain size observed of 23 μm and slightly smaller than the largest cut-point for the cascade impactor. The smaller particles are generated due to the crack branching mechanism. After fifteen minutes, the distribution shifts and those fragments remaining in the air have a length (s_0 = 3.84 μm) corresponding to the crack branch penetration depth on detonation (λ = 3.92 μm).

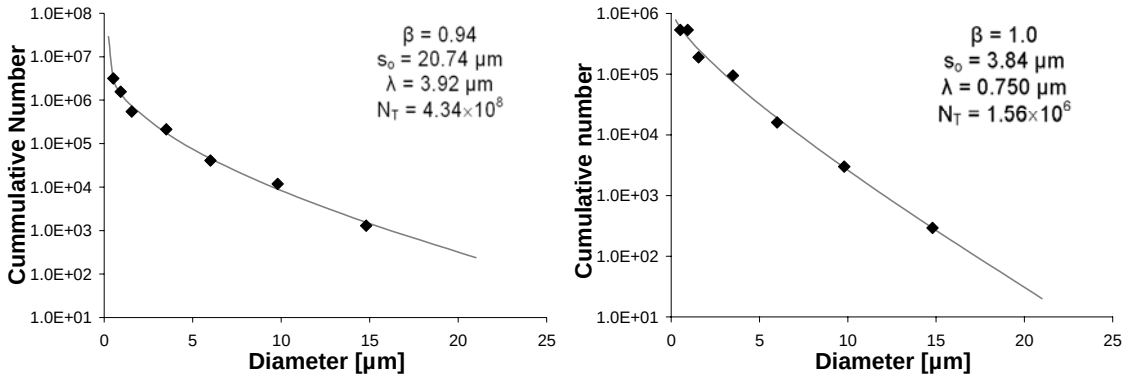

(a) (b)

Figure 4. The cumulative number aerosol distributions as a function of particle size for cerium dioxide for the five minute period (a) immediately after detonation and (b) starting fifteen minutes after detonation.

For the fragment sizes considered here, the fragment distribution is related to the grain size of the parent material. The large particles have dimensions similar to the smaller grain sizes in the microstructure, and result from intergranular fracture. The particles that remain airborne are generated through the crack branching mechanism in the individual grains and result from transgranular fracture. The two materials have similar values for the Young' modulus but cerium dioxide has a larger grain size. More elastic energy can be stored per grain and this stored energy fuels crack propagation and branching. The crack branching mechanism results in a significant number of particles in the range of 3 to 5 μm, which is reflected in the model by a lower value of β. The strontium titanate has smaller grains, storing less energy and thus fewer smaller fragments are generated on explosive fracture.

The size of these fragments is also influenced by the fracture toughness of the materials. The fracture toughness of strontium titanate is 1.0 MPa $m^{½}$ [9] and that of cerium dioxide is 1.4 MPa $m^{½}$ [10]. Comparing the ratio of toughness to the ratio of the penetration depth of strontium titanate, 1.24 μm, to that cerium dioxide, 3.92 μm, the ratios are qualitatively correct.

5. SUMMARY

Initial results on ceramic fracture and fragment size distribution under explosive loads have been presented. There is some evidence of fragment agglomeration in the debris cloud. The grain size of the parent material plays a significant role in the resulting fragment distribution. The fragments that remain airborne are generated through crack branching mechanisms within the grains of the material. This mechanism is facilitated by a larger grain size.

6. ACKNOWLEDGEMENTS

The authors acknowledge the contributions of M. Chan and T. Troczynski of the University of British Columbia in materials preparation and characterization and the contribution of J. Murimboh of Acadia University in providing the scanning electron microscope images.

7. REFERENCES

[1] R. H. Richards, C. E. Locke, *Textbook of Ore Dressing*, 3rd edition. McGraw-Hill book company, Inc. New York and London, 1940.
[2] H. Inaoka, E. Toyosawa, and H. Takayasu, Aspect Ratio Dependence of Impact Fragmentation, *Phys. Rev. Lett.* **78**, 3455 (1997).
[3] F. Wittel, F. Kun, H.J. KunHerrmann, and B. H. Kroplin, Breakup of Shells Under Explosion and Impact, *Phys. Rev. E* **71**, 016108 (2005).
[4] H. Katsuragi, S. Ihara, and H. Honjo, Explosive Fragmentation of a Thin Ceramic Tube using Pulsed Power, *Phys Rev Lett*, **95**, 095503, (2005).
[5] E.S.C. Ching, S. L. Lui, and K. Q. Xia, Energy Dependence of Impact Fragmentation of Long Glass Rods, *Physica A*: **287A**, 83 (2000)
[6] D.W. Richardson, *Modern ceramic engineering: properties, processing and use in design*, New York, 1982.
[7] J.A. Åström, R.P. Linna, J. Timonen, P.F. Møller, L Oddershede, Exponential and power-law mass distributions in brittle fragmentation, *Phys Rev E*, **70**, 026104 (2004).
[8] J.A. Åström, F. Ouchterlony, R.P. Linna, J. Timonen, Universal dynamic fragmentation in D dimensions, Phys Rev Lett, **92**, 245506, (2004).
[9] E.A. Giess et al, Lanthanide gallate perovskite-type substrates for epitaxial, high-T_c superconducting $Ba_2YCu_3O_{7-\delta}$ films, *IBM J Res Develop*, **34**, 916-926 (1990).
[10] S. Maschio, O. Sbaizero, S. Meriani, Mechanical properties in the ceria-zirconia system, *J Eur Ceram Soc*, **9**, 127-132 (1992).